Salt anisotropy: Ultrasonic lab experiments and traveltime ramifications

Jingjing Zong, Robert Stewart and Nikolay Dyaur*
University of Houston

Summary

Salt plays an important role in the Gulf of Mexico and other areas of the world. In the previous laboratory measurements, it has shown cubic anisotropy on halite (rock salt). For salt formation in the Gulf of Mexico, the deformation and the flow of evaporates could lead to the realignment of constituent crystals which also generates anisotropic aggregates (Raymer *et al.*, 2000). In this paper, we investigate and quantify anisotropy of pure halite. With respect to all polarization in the pure halite, Vp changes from 4.44 to 4.76 km/s and Vs changes from 2.47 to 2.92 km/s. The difference of the one-way travel time caused by this cubic anisotropy for a 1km thick 3D numerical model is up to 0.02s, 0.06s and 0.03s and for P wave, SV wave and SH wave, respectively.

Introduction

Salt has generally been treated as isotropic in regular seismic process for years. However, with more attention attached to subsalt imaging, it is essential to fully understand the salt properties. Our work contains two parts: one is the ultrasonic lab measurement of pure halite and another is the numerical modeling of pure salt in the field scale. The lab measurements are consistent with pure halite crystals, showing the cubic symmetry. The shear-wave splitting and compressional wave variations support the cubic symmetry definition. Furthermore, numerical models are built to investigate reflections as well as the travel time differences caused by the cubic anisotropy. First, we built two numerical velocity models: one basic model which has three isotropic layers, and another anisotropic model with the second layer substituted by pure salt. The anisotropy parameters are calculated from our laboratory measurements. We further built a single layer model to quantify the travel time difference caused by the cubic anisotropy.

Salt anisotropy theory

Salt was treated as an isotropic medium mainly because of its weak variation in velocity. When salt shows seismic anisotropy, it may be generated from three aspects: the nature of salt crystal (halite), which, orientated fractures the flowage of salt. In this paper, we study the nature of pure salt to investigate the cubic anisotropy.
The crystal structure of pure halite salt belongs to cubic symmetry class (Pauling, 1929). Cubic anisotropy is optically isotropic but acoustically anisotropic with 3 independent elastic constants: C_{11}, C_{44}, C_{12} (Slaughter, 2002).
One prominent phenomenon of the anisotropy is shear-wave splitting. The particle motion of shear wave is normal to its propagation direction. In anisotropic media, the shear wave split into two waves with orthogonal particle motion, each traveling with the velocity determined by the stiffness in that direction (Sondergeld and Rai, 1992).
Our ultrasonic measurement uses shear-wave transducers, one source and one receiver. We monitor and quantify the shear-wave splitting to investigate salt's anisotropy and to calculate the anisotropy parameters.

Ultrasonic lab experiments

1) Experimental setup

The experiments are shear and compressional wave ultrasonic transducers (500 kHz), a bench-top device which is designed for fixing sample and controlling azimuthal test, and an azimuthal pointer. Samples are put in between of two transducers with good coupling and cementation (Figure1).

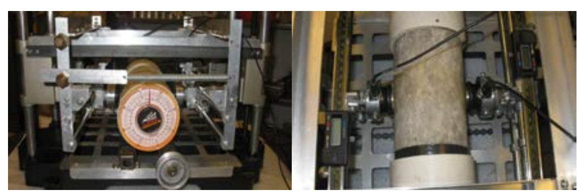

Figure 1. Experimental setup of ultrasonic measurements

By rotating transduces or samples themselves, we can measure the sample with full azimuth. A circular protractor is used to determine the azimuth of rotation. Data are recorded every 10° per trace (from 0° to 360°) with 37 traces per record.
The amplified data are sampled by 0.5MHz using digital oscilloscope which is connected to Multi Channel software.

2) Salt Samples

The test sample is salt crystal from Sifto's Goderich Mine, Canada. The Goderich Mine lies in the northwest of the Michigan basin to and the southeast the Appalachian basin. The salt deposits in Goderich areas are on the east flanks of the Michigan basin and formed part of the Michigan basin salt basin deposits (Hewitt, 1962). The salt deposits at Goderich are from an ancient sea bed of Silurian age, part of Salina Formation(Steele and Haynes, 2000). This salt crystal grew in a very stable environment (located at the depth of 1675-1755 feet). It is remarkably pure, colorless to white, containing less than 2% impurities (Hewitt, 1962). The crystallographic orientation is clear with slight external fractures, which have negligible effect on our measurement.

3) Cubic Symmetry

The three symmetry axes of the salt crystal sample could be identified clearly by human eye. Later on, the results indicate there is a slight deviation with Z axis, which comes from the error during preparation. In the experiment, I use Miller indices convention, defining symmetry direction X,Y,Z as (1,0,0),(0,1,0),(0,0,1), respectively.

The experiment on salt crystal samples includes two parts:

a. With shear wave propagating along the symmetry axes XYZ respectively <1,0,0>([1,0,0],[0,1,0],[0,0,1]) (Figure 2).
b. With shear wave propagating in the direction halfway between symmetry axes (Y and Z) normal to plane (0,1,1), (Figure 3).

For part 1, taking the X axis for example, we put the transducers facing YOZ plan so that the shear wave propagates in X direction. We rotate the transducers synchronously from 0° to 360° with a 10° increment. The same configuration is applied to other Y and Z.

Figure 4 shows our shear wave first arrivals in all polarization direction from 0° to 360°. There is no time shift of shear wave first arrivals, indicating our results from actual observation agree with the wave theory for cubic symmetric crystal that the shear waves have the same velocity along the principle or symmetry axes. Vp and Vs are constant in three symmetries, 4.75 and 2.46 km/s respectively. It is the maximum velocity. The Vp/Vs is 1.93. The slight variation of first arrivals for shear wave propagating along Z axis is supposed to be caused by error when prepare the sample. Errors could happen when the Z axis we choose are not the exact symmetry. The error also confirms the property that all shear wave records are expected to show splitting except on symmetry axes in cubic symmetric crystal samples.

For the second part, we have shear wave propagating halfway (45°) between Y and Z and normal to plane YOZ (0,1,1). Both shear wave transducers are rotated synchronously from polarization 0° to 360° with 10° increment. Figure 5 shows shear-wave splitting with respect to polarization, featured with period of 180° for the two shear wave. The fast Vs is 2.92 km/s while the slow Vs is 2.47 km/s. The distinctive velocity variation is 18.22%. In this direction, Vp decreases to 4.44 km/s, with 7.2% variation compared to Vp in three symmetries. This is an important feature of wave propagating in anisotropic media. The anisotropy we observed here is confirmed to be the result of crystal alignment, rather than post-excavation effects. The minor fractures growing inside the salt sample do not affect our result. The velocities in three symmetry axes are consistent with each other.

Since we have the velocities in three symmetries and one more set of velocity at 45^0 between two symmetries. We can calculate the cubic elastic constants as well as the anisotropy parameters. C_{11} and C_{44} are solved from Vp and Vs in the symmetry axes, respectively. C_{12} is calculated by the velocities in the halfway between two symmetries. Finally, we have $C_{11} = 48.74$, $C_{44} = 13.07$, $C_{12} = 12.648$ .The theoretical phase-velocity surfaces on symmetry planes for 4 quadrants are computed (Figure 6). Both P and fast S velocity are changing off the symmetry. They reach the maximum in the halfway of two symmetry axes. The variation is symmetric.

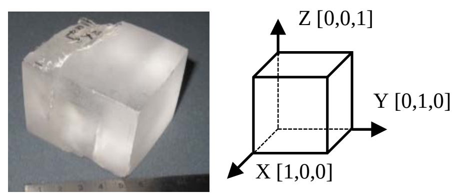

Figure 2. Cubic salt crystal sample and the three symmetry axes X, Y, Z <1,0,0> ([1,0,0],[0,1,0],[0,0,1]).

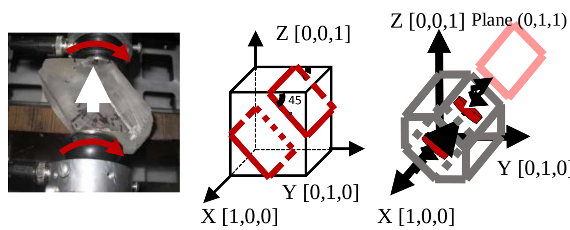

Figure 3. a. Salt crystal sample ready for measurement. b. Diagram to show that how the sample is cut. c. Diagram to show shear wave propagating in the direction halfway between axes Y and Z.

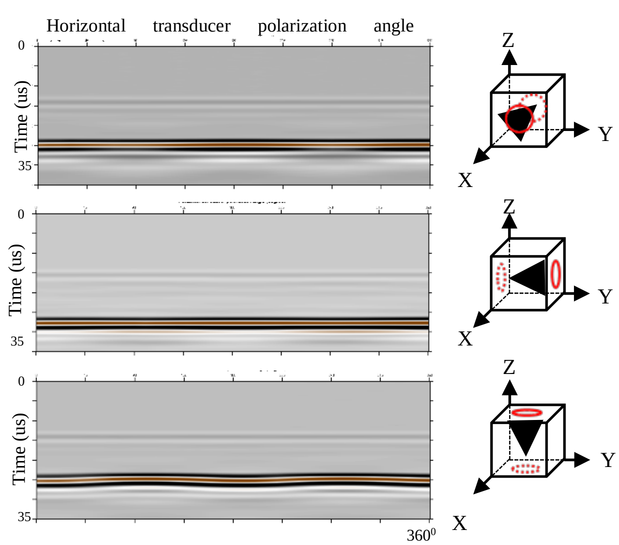

Salt anisotropy: Ultrasonic lab experiments and traveltime ramifications

	Vp(km/s)	Vs(km/s)	Vp/Vs
X	4.75	2.46	1.93
Y	4.75	2.46	1.93
Z	4.76	2.46	1.94

Figure 4. Left plot shows first arrivals of cubic crystal sample in all polarization direction from 0° to 360° in X, Y and Z axes. Right plot shows the diagrams of three propagation directions. Bottom plot shows the velocities calculated from first arrivals.

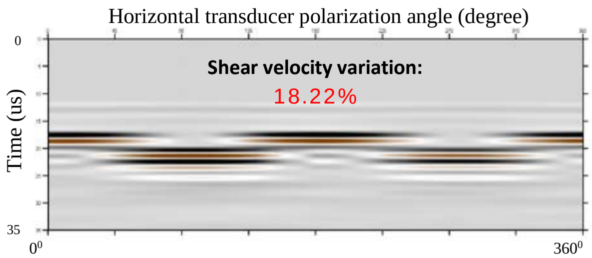

Vp(km/s)	Vs(km/s)	Vp/Vs
4.44	S1:2.92	1.52
	S2:2.47	1.80

Figure 5. Upper plot shows shear wave first arrivals of crystal sample in all polarization direction from 0° to 360° in halfway between Y and Z. Bottom table shows the velocities and anisotropy parameters calculated from first arrivals.

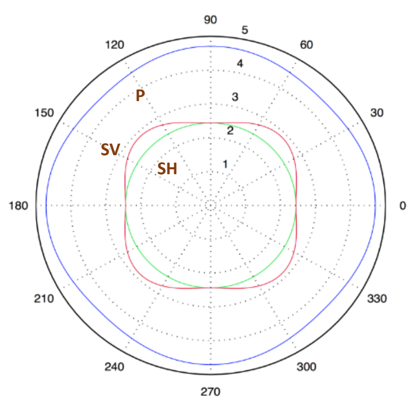

Figure 6. Phase velocity surfaces in 4 quadrants on symmetry plane.

Numerical modeling

1) Reflection of cubic anisotropic media

The reflection of anisotropic media is expected to be different from the isotropic one. With the elastic constants changing, shear wave splitting is expected in anisotropic media.

a. Three isotropic layers (model 1)

We first built a three-layer model with each layer being isotropic and homogeneous (Figure 7). The first layer is 0.5km thick, density=2.2g/cm^3, Vp=2km/s, Vs=1km/s. The second layer is 1.5km thick, density=2.16g/cm^3, Vp=4.75km/s, Vs=2.46km/s. The third layer is infinite thick, density=2.2g/cm^3, Vp=2km/s, Vs=1km/s. Our parameters for second layer come from the lab measurements of pure salt. Reflections of the interfaces are computed by Anivec software package (Figure 8). The source and receivers are put on the surface. Source is in the middle and offset is from -3000m to 3000m, 10m interval. The hyperbolic curves are reflections and the straight lines are direct wave. From the reflections, we can clearly separate P wave, converted wave and S wave. The velocity of converted wave is larger than S velocity and smaller than P velocity. Reflective energy of the second interface is much weaker than the first one which is the result of very high velocity contrast of the first two layers. In this isotropic three-layer model, we do not see any shear-wave splitting.

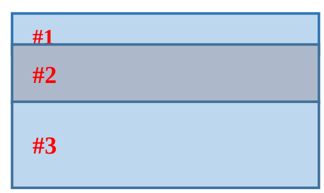

Figure 7. Three layers model.
Model 1: #1 0.5km, Vp=2km/s, Vs=1km/s, ρ=2.2g/cm^3, #2 1.5km,Vp=4.75km/s, Vs=2.46km/s, ρ=2.16g/cm^3, #3 Infinite, Vp=2km/s, Vs=1km/s, ρ=2.2g/cm^3
Model 2: #1 0.5km, Vp=2km/s, Vs=1km/s, ρ=2.2g/cm^3, #2 1.5km, salt layer, $C_{11} = 48.74, C_{44} = 13.07, C_{12} = 12.648$, #3 Infinite, Vp=2km/s, Vs=1km/s, ρ=2.2g/cm^3

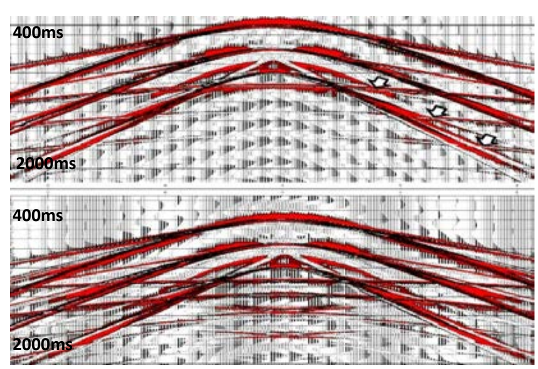

Figure 8. Reflection of three layered model. Upper plot is the reflections of model 1. Lower plot is the reflections of model 2.

b. Salt layer embedded (model 2)

We further built another model with the second layer substituted by the salt crystal, comparing to the isotropic three-layer model. The anisotropic parameters are calculated: $C_{11} = 48.7, C_{44} = 13.1, C_{12} = 12.6$.
The geometry is same as model 1. The reflection of this model is much more complex than the first one (Figure 8). The converted shear wave and S wave both split in the second layer. We can see four different reflected velocities except for P wave velocity. We subtract the P wave for a clear view of shear-wave splitting. As marked in Figure 8, those hyperbolas are fast converted wave, slow converted wave, fast S wave and slow S wave successively (Figure 9).

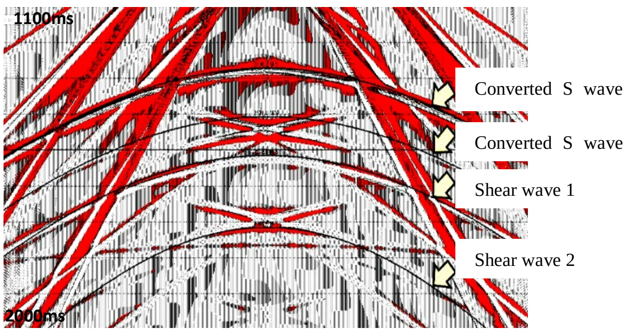

Figure 9. Subtract P wave from the reflection of model 2.

2) Travel time difference caused by cubic anisotropy

In order of comparing with field data, our ultrasonic measurements for the salt sample need to be upscaled. For the purpose of quantifying the travel time difference caused by cubic anisotropy in larger scale, we calculate travel time for 1 km isotropic single-layer 3D model and another anisotropic (cubic symmetry) one respectively. The transient time is calculated for this 3D single-layer model (Figure 10). The source is set at point A while receivers are on the bottom surface. The ray sweep is controlled by angle. The ray path covers a quarter cycle crone when φ sweeps from 0° to 45° and θ from 0° to 90°. For the isotropic layer, we use Vp=4.75 km/s and Vs=2.46 km/s, the same as what we measured in cubic symmetry axes. The travel time is easily calculated by dividing velocity from travel distance. For the cubic anisotropic media, we have three independent elastic constants: C_{11}, C_{44}, C_{12} . Phase velocities, group velocities and causative travel time could be calculated by using Green Christoffel equation. From the difference of travel time for the two media, we can see the variance in different polarization direction. In the cubic anisotropic media, the one way travel time difference reaches the maximum in the halfway between two symmetry axes and the minimum in the symmetry axes. For 1 km depth, one way time difference for the two models is up to 0.02s, 0.03s and 0.06s for P wave, SH wave and SV wave respectively. The ramifications of treating pure salt as isotropic media are shown in Figure 10.

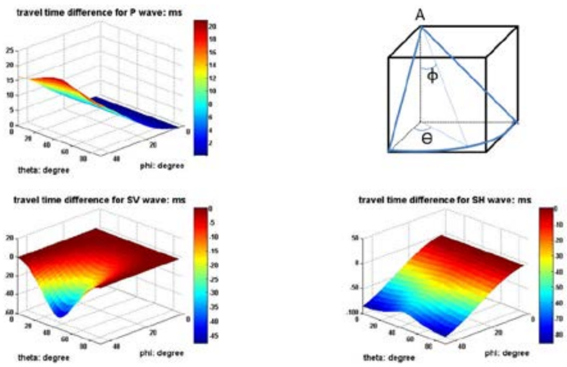

Figure 10. Travel time difference caused by cubic anisotropy. The first three plots are travel time difference of P, SV and SH wave respectively. The last plot is the ray path coverage of the simple layer 3D model.

Conclusion

From the ultrasonic lab measurements, we confirmed the velocity variation and shear-wave splitting in the directions away from the symmetry axes. Our numerical results also agree with the theory for cubic symmetry that velocities along symmetry axes are constant while P wave decreasing and shear wave splitting in other directions. The variation reaches maximum in the halfway between two symmetry axes. The one way travel time difference for 1 km thick block provides collation for ignoring such cubic anisotropy in processing. Current results provide reference for the influence of cubic salt in seismic processing.

Acknowledgement

We would also like to thank all the Allied Geophysics Laboratory (AGL) personal and sponsors for their assistant in this project.

Hewitt, D.F., 1962. *Salt in Ontario*, edn, Vol., pp. Pages, F. Fogg, printer to the Queen.

Pauling, L., 1929. The principles determining the structure of complex ionic crystals, *Journal of the American Chemical Society*, 51**,** 1010-1026.

Raymer, D., Kendall, J., Pedlar, D., Kendall, R., Mueller, M. & Beaudoin, G., 2000. The significance of salt anisotropy in seismic imaging. *in Proceedings of 70th Annual Int. Meeting of the Soc. Explor. Geophys., Calgary*.

Slaughter, W.S., 2002. *The linearized theory of elasticity*, edn, Vol., pp. Pages, Springer.

Sondergeld, C. & Rai, C., 1992. Laboratory observations of shear-wave propagation in anisotropic media, *The leading edge*, 11**,** 38-43.

Steele, K. & Haynes, S.J., 2000. Mines and wines: Industrial minerals, geology and wineries of the Niagara region, field trip guidebook.